Hindawi Publishing Corporation
EURASIP Journal on Audio, Speech, and Music Processing
Volume 2009, Article ID 876297, 16 pages
doi:10.1155/2009/876297

Research Article

Signal Processing Implementation and Comparison of Automotive Spatial Sound Rendering Strategies

Mingsian R. Bai and Jhih-Ren Hong

Department of Mechanical Engineering, National Chiao-Tung University, 1001 Ta-Hsueh Road, Hsin-Chu 300, Taiwan

Correspondence should be addressed to Mingsian R. Bai, msbai@mail.nctu.edu.tw

Received 9 September 2008; Revised 22 March 2009; Accepted 8 June 2009

Recommended by Douglas Brungart

Design and implementation strategies of spatial sound rendering are investigated in this paper for automotive scenarios. Six design methods are implemented for various rendering modes with different number of passengers. Specifically, the downmixing algorithms aimed at balancing the front and back reproductions are developed for the 5.1-channel input. Other five algorithms based on inverse filtering are implemented in two approaches. The first approach utilizes binaural (Head-Related Transfer Functions HRTFs) measured in the car interior, whereas the second approach named the point-receiver model targets a point receiver positioned at the center of the passenger's head. The proposed processing algorithms were compared via objective and subjective experiments under various listening conditions. Test data were processed by the multivariate analysis of variance (MANOVA) method and the least significant difference (Fisher's LSD) method as a *post hoc* test to justify the statistical significance of the experimental data. The results indicate that inverse filtering algorithms are preferred for the single passenger mode. For the multipassenger mode, however, downmixing algorithms generally outperformed the other processing techniques.

1. Introduction

With rapid growth in digital telecommunication and display technologies, multimedia audiovisual presentation has become reality for automobiles. However, there remain numerous challenges in automotive audio reproduction due to the notorious nature of the automotive listening environment. In car interior, the confined space lacks natural reverberations. This may degrade the perceived spaciousness of audio rendering. Localization of sound images may also be obscured by strong reflections from the window panels, dashboard, and seats [1]. In addition, the loudspeakers and seats are generally not in proper positions and orientations, which may further aggravate the rendering performance [2, 3]. To address these problems, a comprehensive study of automotive multichannel audio rendering strategies is undertaken in this paper. Rendering approaches for different numbers of passengers are presented and compared.

In spatial sound rendering, binaural audio lends itself to an emerging audio technology with many promising applications [4–10]. It proves effective in recreating stereo images by compensating for the asymmetric positions of loudspeakers in car environment [1]. However, this approach suffers from the problem of the limited "sweet spot" in which the system remains effective [7, 8]. To overcome this limitation, several methods that allow for more accurate spatial sound field synthesis were suggested in the past. The Ambisonics technique originally proposed by Gerzon is a series of recording and replay techniques using multichannel mixing technology that can be used live or in the studio [11]. The Wave Field Synthesis (WFS) technique is another promising method to creating a sweet-spot-free rendering environment [12–14]. Nevertheless, the requirement of large number of loudspeakers, and hence the high processing complexity, limits its implementation in practical systems.

Notwithstanding the eager quest for advanced rendering methods in academia, the majority of the off-the-shelf automotive audio systems still rely on simple systems with panning and equalization functions. For instance, Pioneer's (Multi-Channel Acoustic Calibration MCACC) system attempts to compensate for the acoustical responses between the listener's head position and the loudspeaker by using

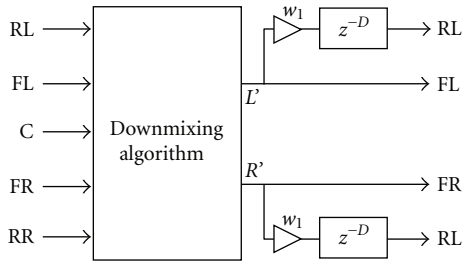

Figure 1: The block diagram of the downmixing with weighting and delay (DWD) method.

a 9-band equalizer [15]. Rarely has been seen a theoretical treatment with rigorous evaluation on the approaches that have been developed for this difficult problem.

If binaural audio and the WFS are regarded as two extremes in terms of loudspeaker channels, this paper is focused on pragmatic and compromising approaches of automotive audio spatializers targeted at economical cars with four available loudspeakers for 5.1-channel input contents. In these approaches, it is necessary to downmix the audio signals to decrease the number of audio channels between the inputs and the outputs [16]. By combining various inverse filtering and the downmixing techniques, six rendering strategies are proposed for various passengers' sitting modes. One of the six methods is based on downmixing approaches, whereas the remaining five methods are based on inverse filtering.

The proposed approaches have been implemented on a real car by using a fixed-point digital signal processor (DSP). Extensive objective and subjective experiments were conducted to compare the presented rendering strategies for various listening scenarios. In order to justify the statistical significance of the results, the data of subjective listening tests are processed by the multivariate analysis of variance (MANOVA) [17] method, followed by the least significant difference method (Fisher's LSD) as a *post hoc* test. In light of these tests, it is hoped that viable rendering strategies capable of delivering compelling and immersive listening experience in automotive environments can be found.

2. Downmixing-Based Strategy

In this section, rendering strategy based on downmixing is presented. Given 5.1-channel input contents, a straightforward approach is to feed the input signals to the respective loudspeakers. However, this approach often cannot deliver satisfactory sound image duo to the asymmetric arrangement of the loudspeakers/passengers in the car environment. To balance the front and back, the downmixing with weighting and delay (DWD) method is developed, as depicted in the block diagram of Figure 1. According to the standard downmixing algorithm stated in ITU-R BS.775-1 [18], the center channel is weighted by 0.71 (or -3 dB) and mixed into the frontal channels. Similarly, the back left and the back right surround channels are weighted by 0.71 and mixed into the front left and the front right channels, respectively. That is,

$$\begin{aligned} L &= \mathrm{FL} + 0.71 \times \mathrm{C} + 0.71 \times \mathrm{BL} \\ R &= \mathrm{FR} + 0.71 \times \mathrm{C} + 0.71 \times \mathrm{BR}. \end{aligned} \tag{1}$$

Next, the frontal channels are weighted (0.65) and delayed (20 millisecond) to produce the back channels.

3. Inverse Filtering-Based Approaches

Beside the aforementioned downmixing-based strategy, five other strategies are based on inverse filtering. These design strategies are further divided into two categories. The first category is based on the Head-Related Transfer Functions (HRTFs) that account for the diffraction and shadowing effects due to the head, ears, and torso. Three rendering strategies are developed to reproduce four virtual images located at $\pm 30^\circ$ and $\pm 110^\circ$ in accordance with the 5.1 deployment stated in ITU-R Rec. BS.775-1 [18]. For the 5.1-channel inputs and four loudspeakers, the center channel has to be attenuated by -3 dB and mixing into the front-left and the front-right channels. The HRTF database measured by the MIT Media Laboratory [19, 20] is employed as the matching model, whereas the HRTFs measured in the car are used as the acoustical plant. The second category named "the point-receiver model" regards the passenger's head as a simple point-receiver at the center.

3.1. Multichannel Inverse Filtering. The inverse filtering problem can be viewed from a model-matching perspective, as shown in Figure 2. In the block diagram, $\mathbf{x}(z)$ is a vector of N program inputs, $\mathbf{v}(z)$ is a vector of M loudspeaker inputs, and $\mathbf{e}(z)$ is a vector of L error signals or control points. Also, $\mathbf{M}(z)$ is an $L \times N$ matrix of the matching model, $\mathbf{H}(z)$ is an $L \times M$ plant transfer matrix, and $\mathbf{C}(z)$ is an $M \times N$ matrix of the inverse filters. The z^{-m} term accounts for the modeling delay to ensure causality of the inverse filters. For arbitrary inputs, minimization of the error output is tantamount to the following optimization problem:

$$\min_{\mathbf{C}} \|\mathbf{M} - \mathbf{HC}\|_F^2, \tag{2}$$

where F symbolizes the Frobenius norm [21]. Using Tikhnov regularization, the inverse filter matrix can be shown to be [7].

$$\mathbf{C} = \left(\mathbf{H}^H\mathbf{H} + \beta\mathbf{I}\right)^{-1}\mathbf{H}^H\mathbf{M}, \tag{3}$$

The regularization parameter β that weights the input power against the performance error can be used to prevent the singularity of $\mathbf{H}^H\mathbf{H}$ from saturating the filters. If β is too small, there will be sharp peaks in the frequency responses of the CCS filters, whereas if β is too large, the cancellation performance will be rather poor. The criterion for choosing the regularization parameter β is dependent on a preset gain threshold [7]. Inverse Fast Fourier transforms (FFT) along with circular shifts (hence the modeling delay) are needed to obtain causal FIR filters.

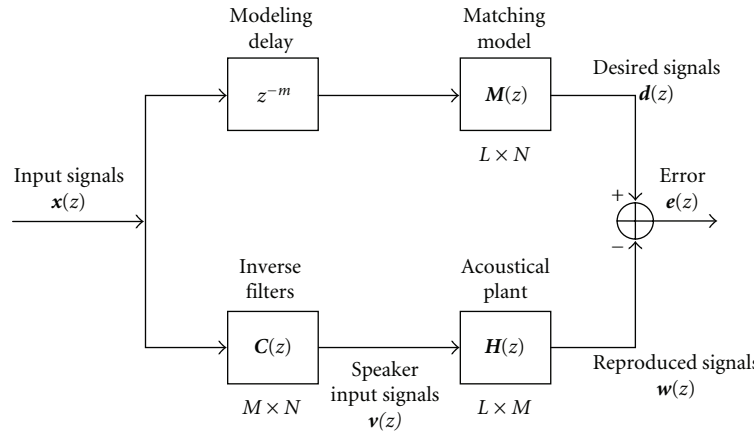

Figure 2: The block diagram of the multichannel model matching problem. L: number of control points, M: number of loudspeakers, N: number of program inputs.

In general, it is not robust to implement the inverse filters based on the measured room responses that usually have many noninvertible zeros (deep troughs) [22]. In this paper, a generalized complex smoothing technique suggested by Hatziantoniou and Mourjopoulos [23] is employed to smooth out the peaks and dips of the acoustical frequency responses before the design of inverse filters.

3.2. Inverse Filtering-Based Approaches and Formulation

3.2.1. HRTF Model. The experimental arrangement for a single passenger sitting on an arbitrary seat, for example, the front left seat, in the car is illustrated as Figure 3. This arrangement involves two control points at the passenger's ears, four loudspeakers, and four input channels. Thus, the 2×4 acoustical plant matrix $\mathbf{H}(z)$ and the 2×4 matching model matrix $\mathbf{M}(z)$ can be written as

$$\mathbf{H}(z) = \begin{bmatrix} H_{11}(z) & H_{12}(z) & H_{13}(z) & H_{14}(z) \\ H_{21}(z) & H_{22}(z) & H_{23}(z) & H_{24}(z) \end{bmatrix}, \tag{4}$$

$$\mathbf{M}(z) = \begin{bmatrix} \mathrm{HRTF}^{i}_{30} & \mathrm{HRTF}^{c}_{30} & \mathrm{HRTF}^{i}_{110} & \mathrm{HRTF}^{c}_{110} \\ \mathrm{HRTF}^{c}_{30} & \mathrm{HRTF}^{i}_{30} & \mathrm{HRTF}^{c}_{110} & \mathrm{HRTF}^{i}_{110} \end{bmatrix}, \tag{5}$$

where the superscripts i and c refer to the ipsilateral and the contralateral paths, respectively. The subscripts 30 and 110 in the matching model matrix $\mathbf{M}(z)$ signify the azimuth angles of the HRTF. The HRTFs are assumed to use symmetry, the $-\mathrm{HRTF}_{30}$ and $-\mathrm{HRTF}_{110}$ are generated by swapping the ipsilateral and contralateral sides of $+\mathrm{HRTF}_{30}$ and $+\mathrm{HRTF}_{110}$. The acoustical plants $\mathbf{H}(z)$ are the frequency response functions between the inputs to the loudspeakers and the outputs from the microphones mounted in the (Knowles Electronics Manikin for Acoustic Research KEMAR's) [19, 20] ears. This leads to a 4×4 matrix inversion problem, which is computationally demanding to solve. In order to yield a more tractable solution, the current research has separated this problem into two parts: the front side and the back side. Specifically, the frontal loudspeakers are responsible for generating the sound images at ±30°, while the back loudspeakers are responsible for generating the sound images at ±110°. In this approach, the plant, the matching model, and the inverse filter matrices are given by

$$\begin{aligned} \mathbf{H}^{F}(z) &= \begin{bmatrix} H_{11}(z) & H_{12}(z) \\ H_{21}(z) & H_{22}(z) \end{bmatrix}, \\ \mathbf{H}^{B}(z) &= \begin{bmatrix} H_{13}(z) & H_{14}(z) \\ H_{23}(z) & H_{24}(z) \end{bmatrix}, \end{aligned} \tag{6}$$

$$\begin{aligned} \mathbf{M}^{F}(z) &= \begin{bmatrix} \mathrm{HRTF}^{i}_{30} & \mathrm{HRTF}^{c}_{30} \\ \mathrm{HRTF}^{c}_{30} & \mathrm{HRTF}^{i}_{30} \end{bmatrix}, \\ \mathbf{M}^{B}(z) &= \begin{bmatrix} \mathrm{HRTF}^{i}_{110} & \mathrm{HRTF}^{c}_{110} \\ \mathrm{HRTF}^{c}_{110} & \mathrm{HRTF}^{i}_{110} \end{bmatrix}, \end{aligned} \tag{7}$$

$$\begin{aligned} \mathbf{C}^{F}(z) &= \begin{bmatrix} C^{F}_{11}(z) & C^{F}_{12}(z) \\ C^{F}_{21}(z) & C^{F}_{22}(z) \end{bmatrix}, \\ \mathbf{C}^{B}(z) &= \begin{bmatrix} C^{R}_{11}(z) & C^{R}_{12}(z) \\ C^{R}_{21}(z) & C^{R}_{22}(z) \end{bmatrix}, \end{aligned} \tag{8}$$

where superscripts F and B denote the front-side and the back-side, respectively. The inverse matrices are calculated using (3). In comparison with the formulation in (4) and (5), a great saving of computation can be attained by applying this approach. The number of the inverse filters reduces from sixteen (one 4×4 matrix) to eight (two 2×2 matrices).

To be specific, there are two $+\mathrm{HRTF}_{30}$–one for the ipsilateral side (HRTF^{i}_{30}) and another for contralateral side (HRTF^{c}_{30}). Both HRTFs refer to the transfer functions between a source positioned at +30° with respect to the head center and two ears. Although the loudspeakers in the car are not symmetrically deployed, the matching model (consisting of $\pm\mathrm{HRTF}_{30}$ and $\pm\mathrm{HRTF}_{110}$) of the inverse filter design in the present study is chosen tom be symmetrical. For the asymmetrical acoustical plants, we can calculate the inverse

filters using (3). The loudspeaker setups are not symmetrical for the front left virtual sound and the front right virtual sound and hence the acoustical plants are not symmetrical. This results in different solutions for the inverse filters.

Next, the situation with two passengers sitting on different seats, for example, the front left and the back right seats, is examined. This problem involves four control points for two passengers' ears, four loudspeakers, and four input channels. Following the steps from the single passenger case, the design of the inverse filter can be divided into two parts. Accordingly, two 4×2 matrices of the acoustical plants, two 4×2 matrices of the matching models, and two 2×2 matrices of the inverse filters are expressed as follows:

$$\mathbf{H}^F(z) = \begin{bmatrix} H_{11}(z) & H_{12}(z) \\ H_{21}(z) & H_{22}(z) \\ H_{31}(z) & H_{32}(z) \\ H_{41}(z) & H_{42}(z) \end{bmatrix},$$

$$\mathbf{H}^B(z) = \begin{bmatrix} H_{11}(z) & H_{12}(z) \\ H_{21}(z) & H_{22}(z) \\ H_{31}(z) & H_{32}(z) \\ H_{41}(z) & H_{42}(z) \end{bmatrix}, \tag{9}$$

$$\mathbf{M}^F(z) = \begin{bmatrix} \mathrm{HRTF}^i_{30} & \mathrm{HRTF}^c_{30} \\ \mathrm{HRTF}^c_{30} & \mathrm{HRTF}^i_{30} \\ \mathrm{HRTF}^i_{30} & \mathrm{HRTF}^c_{30} \\ \mathrm{HRTF}^c_{30} & \mathrm{HRTF}^i_{30} \end{bmatrix},$$

$$\mathbf{M}^B(z) = \begin{bmatrix} \mathrm{HRTF}^i_{110} & \mathrm{HRTF}^c_{110} \\ \mathrm{HRTF}^c_{110} & \mathrm{HRTF}^i_{110} \\ \mathrm{HRTF}^i_{110} & \mathrm{HRTF}^c_{110} \\ \mathrm{HRTF}^c_{110} & \mathrm{HRTF}^i_{110} \end{bmatrix}, \tag{10}$$

$$\mathbf{C}^F(z) = \begin{bmatrix} C^F_{11}(z) & C^F_{12}(z) \\ C^F_{21}(z) & C^F_{22}(z) \end{bmatrix},$$

$$\mathbf{C}^B(z) = \begin{bmatrix} C^R_{11}(z) & C^R_{12}(z) \\ C^R_{21}(z) & C^R_{22}(z) \end{bmatrix}. \tag{11}$$

The subscripts of $\mathbf{H}_{ij}(z)$, are as follows i = 1,2 refers to the left and right ears of the passenger 1, i = 3,4 refers to the left and the right ears of the passenger 2, and j = 1,2,3,4 refers to the four loudspeakers. In the 4×2 matrices $\mathbf{M}^F(z)$ and $\mathbf{M}^B(z)$, the first and second rows are identical to the third and fourth rows. Specifically, the rows 1 and 2 are for passenger 1 while the rows 3 and 4 are for passenger 2. The two HRTF inversion methods outlined in (6)–(8) and (9)–(11) were used to generate the following test.

HRTF-Based Inverse Filtering for Single Passenger. For the rendering mode with a single passenger and 5.1-channel input, the HRTF-based inverse-filtering (HIF1) method is developed. The block diagram is shown in Figure 4. For the 5.1-channel inputs and four loudspeakers, the center channel has to be attenuated by −3 db before mixing into the front-left and the front-right channels. Next, two frontal channels and two back channels are fed to the respective inverse filters. Prior to designing the inverse filters, the acoustical plants

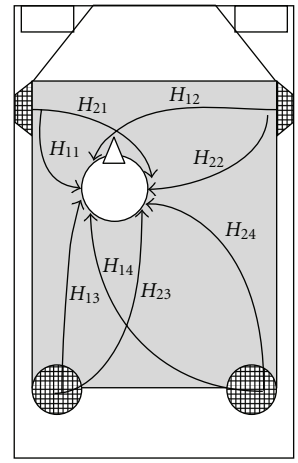

Figure 3: The geometrical arrangement for the HRTF-based rendering approaches.

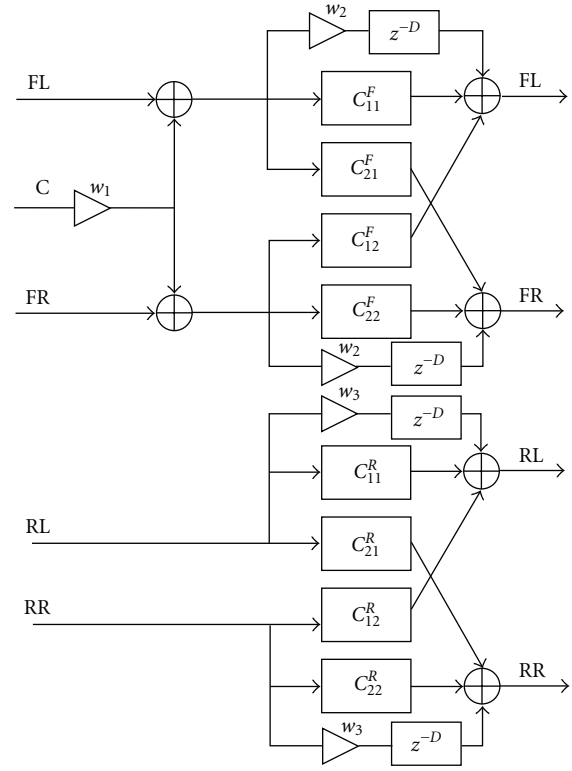

Figure 4: The block diagrams of the HRTF-based inverse filtering for single passenger (HIF1) method, the HRTF-based inverse filtering for two passengers (HIF2) method, and the HRTF-based inverse filtering for two passengers by filter superposition (HIF2-S) method.

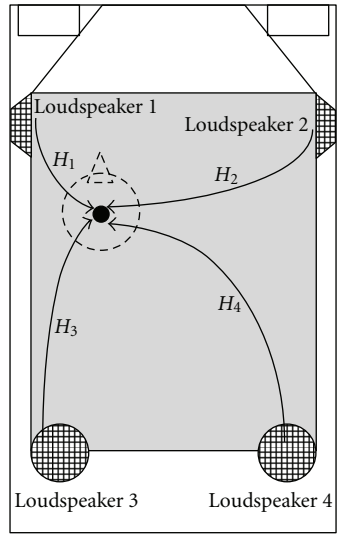

FIGURE 5: The geometrical arrangement for the point receiver-based rendering approaches.

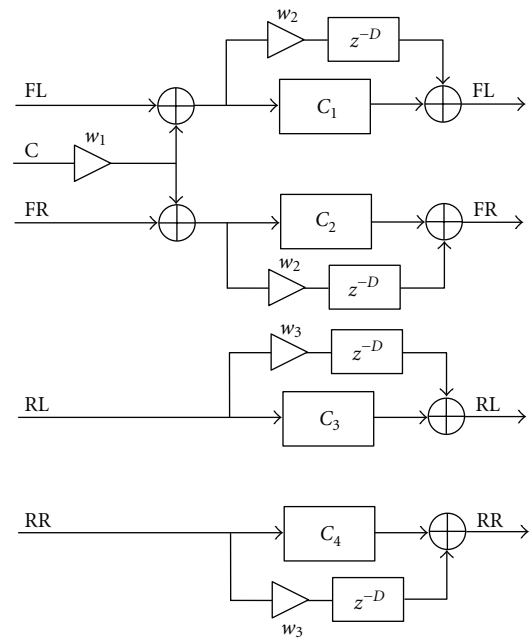

FIGURE 6: The block diagrams of the point-receiver-based inverse filtering for single passenger (PIF1) method and the point-receiver-based inverse filtering for two passengers by filter superposition (PIF2-S) method.

$\mathbf{H}(z)$ in (6) are measured. The matching model matrices and the inverse filters are given in (7) and (8). The weight = 0.45 and delay = 4 ms are used in mixing the four-channel inputs into the respective channels. It is noted that this procedure will also be applied to the following inverse-filtering-based methods.

HRTF-Based Inverse Filtering (HIF2) for Two Passengers. In this section, two HRTF-based inverse filtering strategies designed for two passengers and 5.1-channel input are presented. The first approach named the HIF2 method considers four control points for two passengers. The associated system matrices take the form formulated in (9) to (11). The two 2×2 inverse filter matrices are calculated as previously. The block diagram of the HIF2 method follows that of the HIF1 method.

HRTF-Based Inverse Filtering (HIF2-S) for Two Passengers. In this approach, the inverse filters are constructed by superimposing the filters used in the single-passenger approach. That is

$$\begin{aligned}\mathbf{C}^F_{\text{position 1\&2}}(z) &= \mathbf{C}^F_{\text{position 1}}(z) + \mathbf{C}^F_{\text{position 2}}(z)\\ \mathbf{C}^B_{\text{position 1\&2}}(z) &= \mathbf{C}^B_{\text{position 1}}(z) + \mathrm{C}^B_{\text{position 2}}(z).\end{aligned} \tag{12}$$

This approach is named the HIF2-S method. In (12), the design procedures of the HIF2-S method are divided into two steps. First, the inverse filters for a single passenger sitting on respective positions are designed. Next, by adding the filter coefficients obtained in the first step, two 2×2 inverse filter matrices are obtained. The block diagram of the HIF2-S method follows that of the HIF1 method.

3.2.2. Point-Receiver Model. In this section, a scenario is considered. It is when a single passenger sits on an arbitrary seat in the car, for example, the front left seat, as shown in Figure 5. In this setting, rendering is aimed at what we called the "control point" at the passenger's head center position. A monitoring microphone instead of the KEMAR is required in measuring the acoustical plants and the matching model responses between the input signals and the control points. Hence, the acoustical plant is treated in this approach as four independent (single-input-single-output SISO) systems. These SISO inverse filters can be calculated by

$$C_m(z) = \frac{H_m^*(z)M(z)}{H_m^*(z)H_m(z) + \beta}, \tag{13}$$

where $H_m(z)$, $m = 1 \sim 4$ denotes the transfer function from the mth loudspeaker to the control point. The frequency response function measured using the same type of loudspeakers in the car in an anechoic chamber is designated as the matching model $M(z)$. The point-receiver model was used to generate the following test system.

Point-Receiver-Based Inverse Filtering for Single Passenger. For the 5.1-channel input, the point-receiver-based inverse filtering for single passenger (PIF1) method is developed. This method mimics the concepts of the Pioneer's MCACC [15], but is more accurate in that an inverse filter instead of a simple equalizer is used. The acoustical path from each loudspeaker to the control point is modeled as a SISO system in Figure 5. Four SISO inverse filters are calculated using (13), with identical modeling delay. In Figure 6, the center channel has to be attenuated before mixing into the front-left and front-right channels. The two frontal channels and two back channels are fed to the respective inverse filters.

(a) The 2-liter and 4-door sedan.

(b) The experimental arrangement inside the car equipped with four loudspeakers.

Figure 7: The car used in the objective and subjective experiments.

Table 1: The descriptions of ten automotive audio rendering approaches.

Method	No. input channel	No. passenger	Design strategy
DWD	5.1	1 or more	Downmixing + weighting & delay
HIF1	5.1	1	HRTF-based inverse filtering
HIF2	5.1	2	HRTF-based inverse filtering
HIF2-S	5.1	2	HRTF-based inverse filtering
PIF1	5.1	1	Point-receiver-based inverse filtering
PIF2-S	5.1	2	Point-receiver-based inverse filtering

Point-Receiver-Based Inverse Filtering for Two Passengers. For the rendering scenario with two passengers and 5.1-channel input, the aforementioned filter superposition idea is employed in the point-receiver-based inverse filtering approach (PIF2-S). The structure of this rendering approach is similar to those of the PIF1 approach, as shown in Figure 6. A PIF2 system analogous to the HIF2 system was considered in initial tests, but was eliminated from final testing because the PIF2 approach performed badly in an informal experiment, as compared with the other approaches.

4. Objective and Subjective Evaluations

Objective and subjective experiments were undertaken to evaluate the presented methods, as summarized in Table 1. In the objective experiments, we consider only inverse-filtering based approaches and not downmixing, and we compared the measured inverse-filtering system transfer function with the desired plant transfer function. Through these experiments, it is hoped that the best strategy for each rendering scenario can be found. For the objective experiments, the measurements are only made as HIF1 for the LF listener, HIF2 for the LF and BR listener, and PIF1 for the FL listener, in other words, not all configurations listed in Table 1 were tested objectively. These experiments were conducted in an Opel Vectra 2-liter sedan (Figure 7(a)) equipped with a DVD player, a 7-inch LCD display, a multichannel audio decoder, and four loudspeakers (two mounted in the lower panel of the front door and two behind the back seat). The experimental arrangement inside the car is shown in Figure 7(b). The rendering algorithms were implemented on a fixed-point digital signal processor (DSP), Blackfin-533, of Analog Device semi-conductor. The GRAS 40AC microphone with the GRAS 26AC preamplifier was used for measuring the acoustical plants.

4.1. Objective Experiments

4.1.1. The HRTF-Based Model. In this section, strategies based on the HRTF model are examined. First, for the scenario with a single passenger sitting in the FL seat, the rendering approach of the HIF1 method is examined. Figures 8(a) and 8(b) show the frequency responses of the respective frontal and back plants in the matrix form. The ijth (i = 1,2, and j = 1,2) entry of the matrix figures represents the respective acoustical path in (6). That is, the upper and lower rows of the figures are measured at the left and right ears, respectively. The left and right columns of the figures are measured when the left-side and right-side loudspeakers are enabled, respectively. The measured responses have been effectively smoothed out using the technique developed by Hatziantoniou and Mourjopoulos [23]. Comparison of the left and the right columns of Figures 8(a) and 8(b) reveals that head shadowing is not significant because of the strong reflections from the boundary of the car cabin. The frequency response of the inverse filters show that the filter frequency responses above 6 kHz exhibit high gain because of

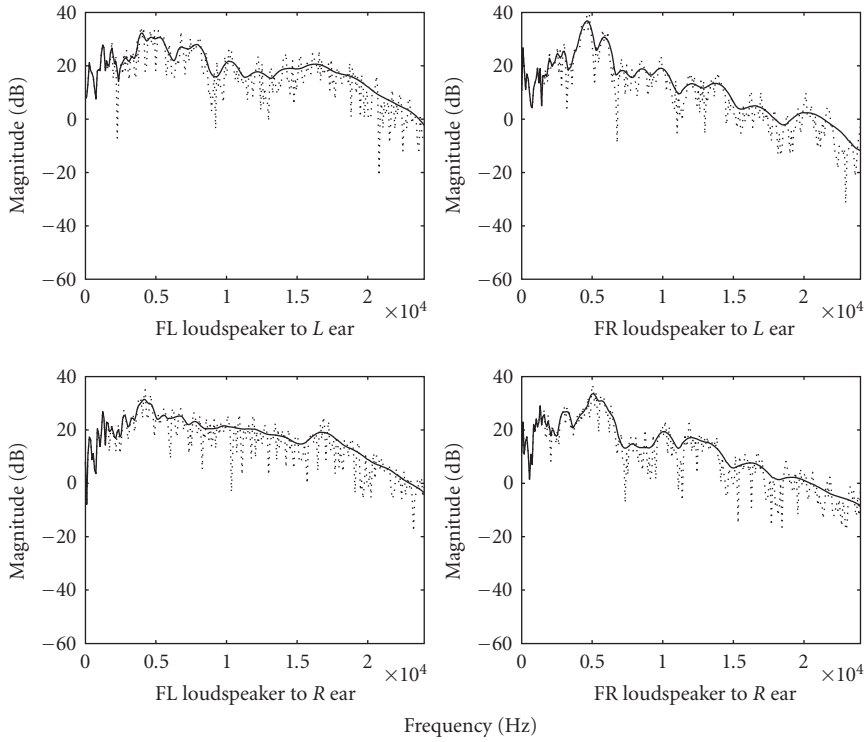

(a) From the frontal loudspeakers.

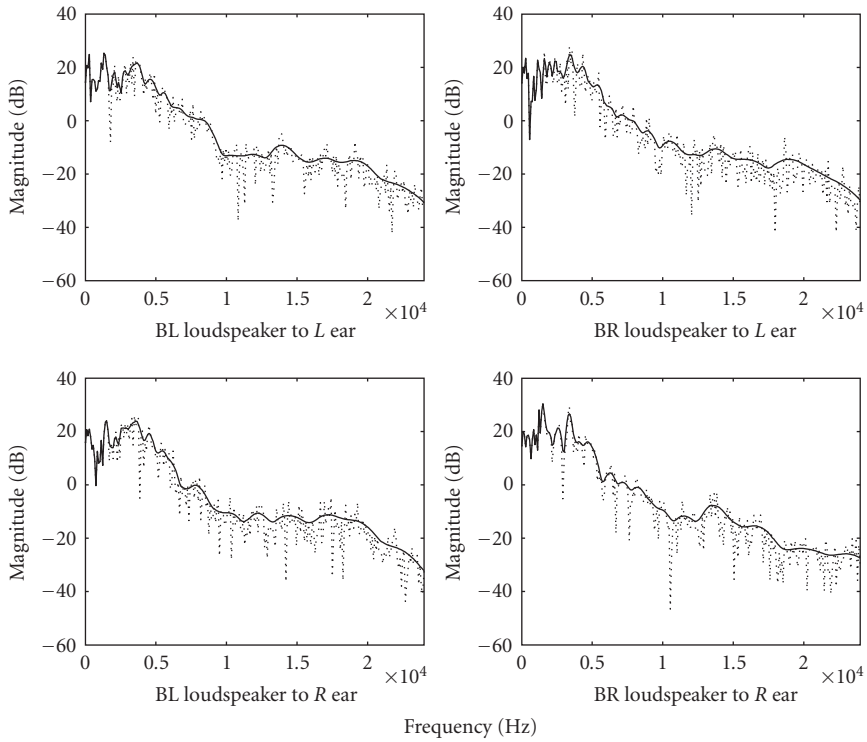

(b) From the back loudspeakers. The dotted lines and the solid lines represent the measured and the smoothed responses.

Figure 8: The frequency responses of the HRTF-based acoustical plant at the FL seat.

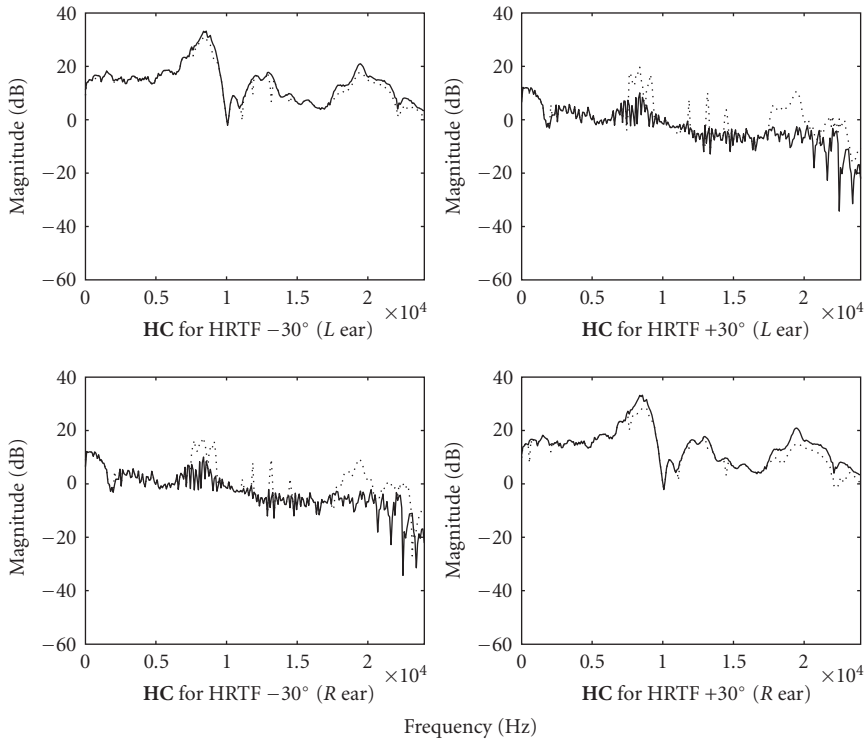

(a) For the frontal image.

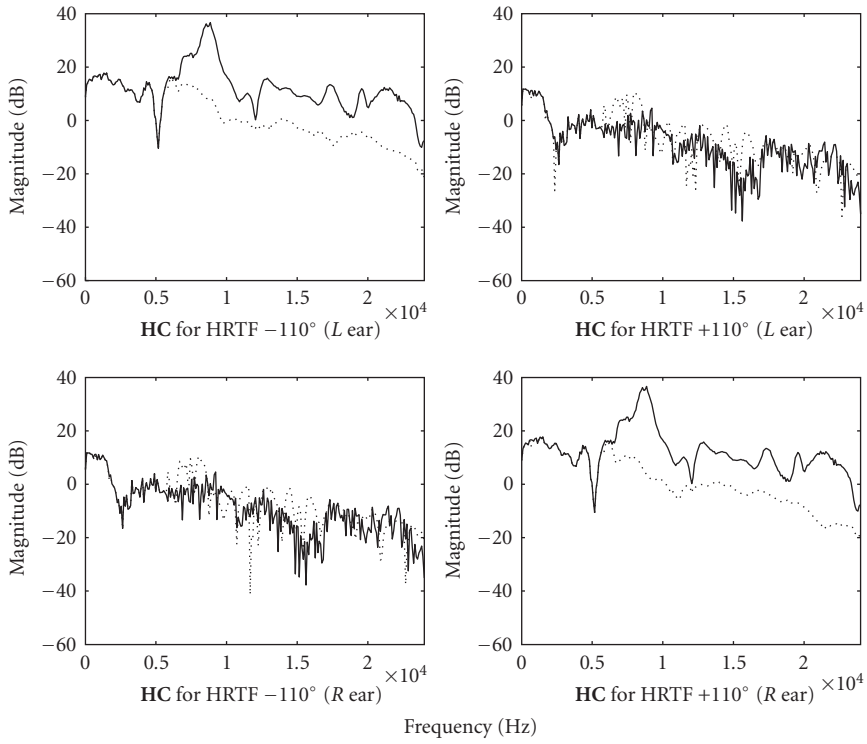

(b) For the back image.

Figure 9: The comparison of frequency response magnitudes of the HRTF-based plant-filter product and the matching model for single passenger sitting in the FL seat. The solid lines and the dotted lines represent the matching model responses **M** and the plant-filter product **HC**, respectively.

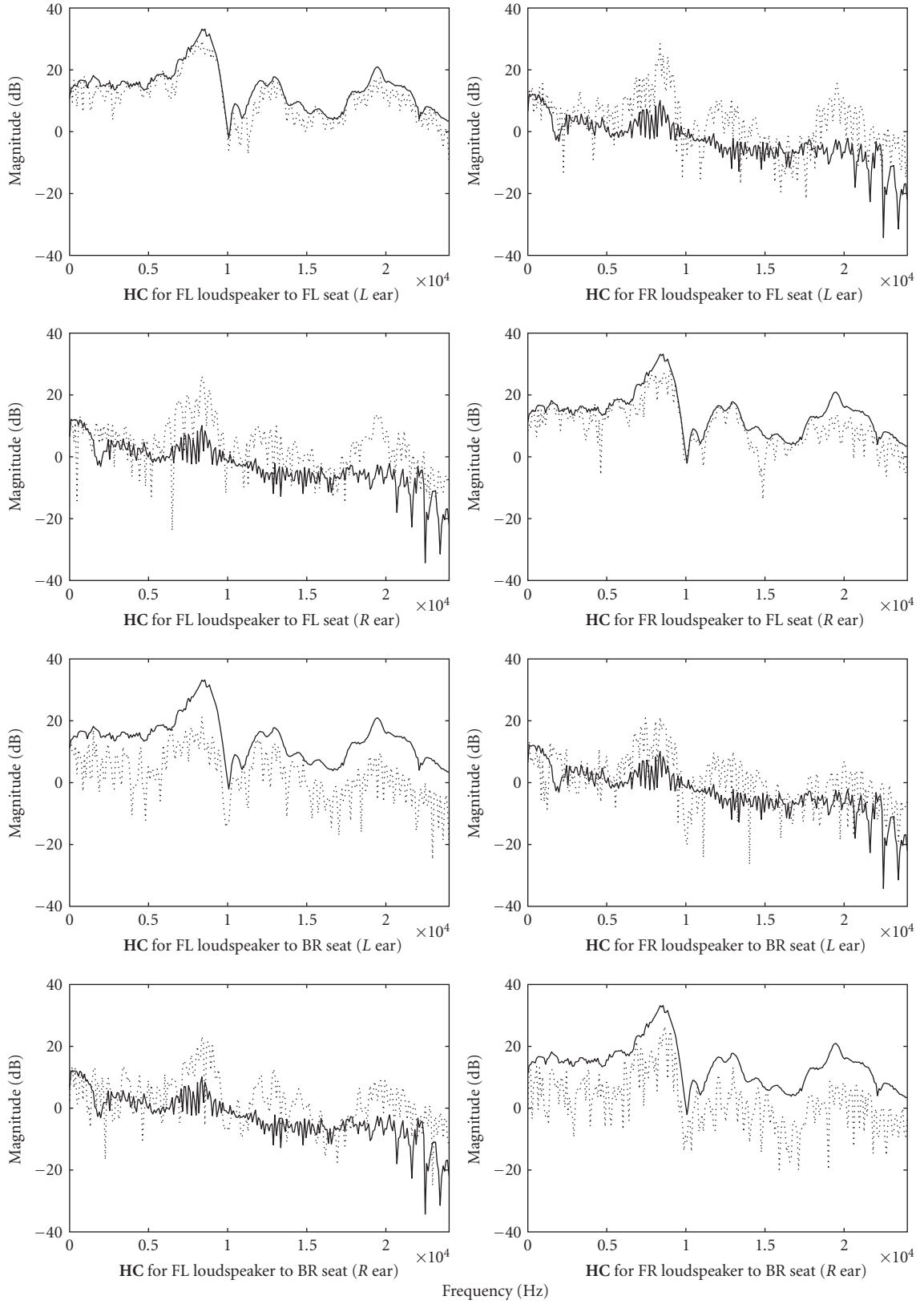

(a) For the frontal image.

Figure 10: Continued.

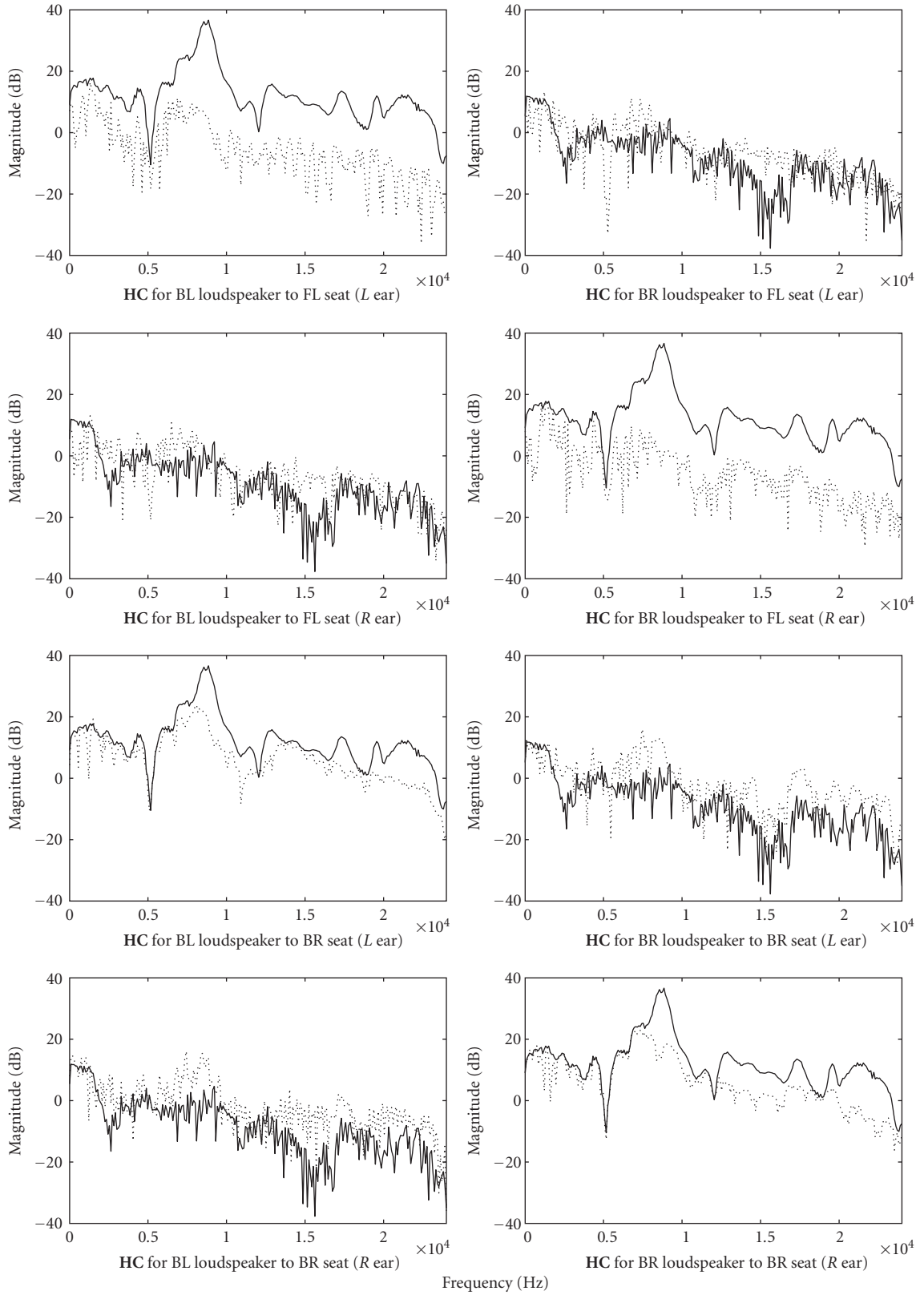

(b) For the back image.

Figure 10: The comparison of frequency response magnitudes of the HRTF-based plant-filter product and the matching model for two passengers sitting in the FL and RR seats. The solid lines and the dotted lines represent the matching model responses **M** and the plant-filter product **HC**, respectively.

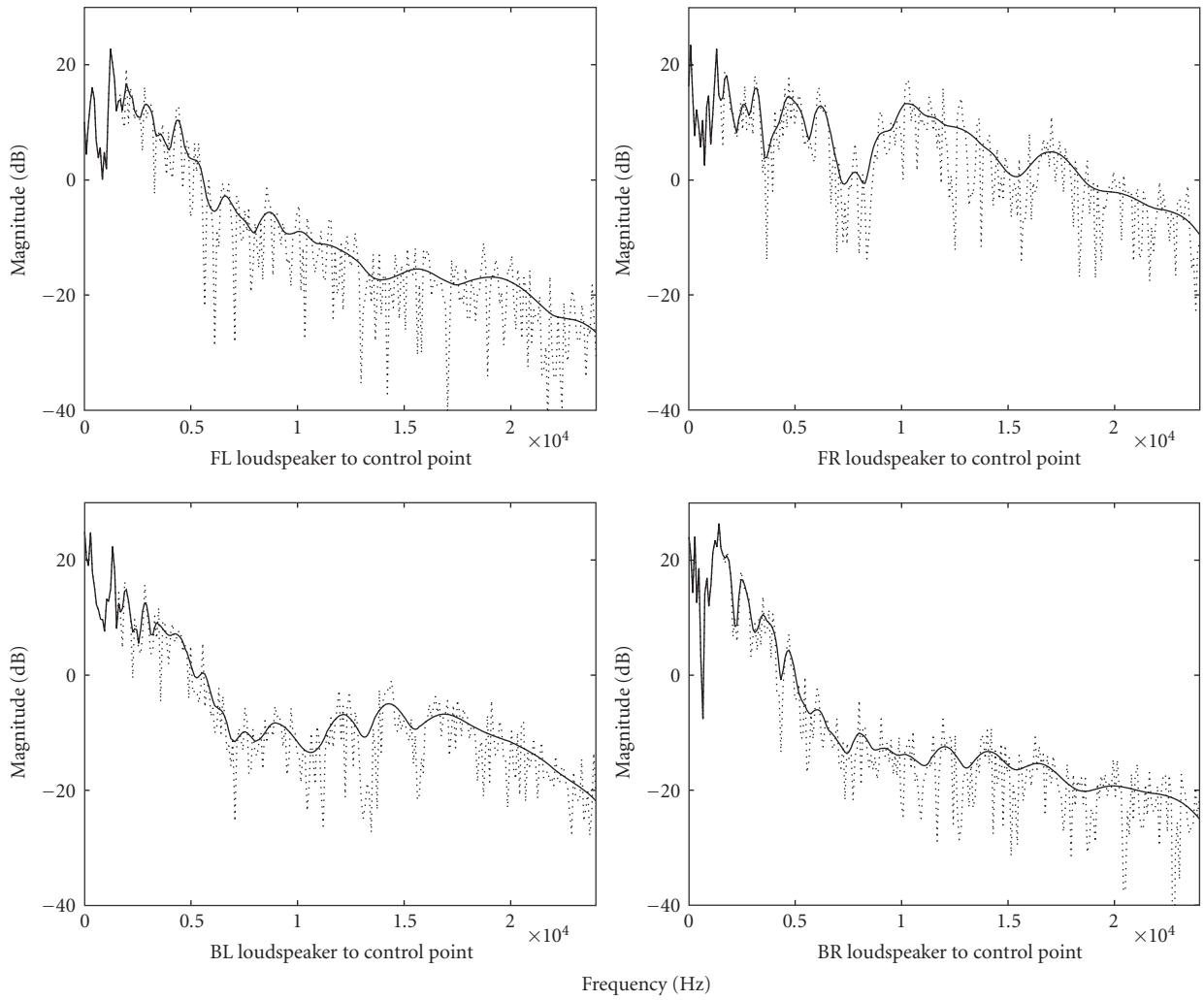

Figure 11: The frequency responses of the point-receiver-based acoustical plants for single passenger sitting in the FL seat. The dotted lines and the solid lines represent the measured and the smoothed responses, respectively.

the poor high-frequency response of the back loudspeakers. To regularize the inverse filters, the gain is always kept below 6 dB to prevent from overloading the loudspeakers. The solid lines in Figures 9(a) and 9(b) represent the HRTF pair at 30° and 110°, respectively, whereas the dotted lines represent the plant-filter product, $\mathbf{H}(e^{j\omega})\mathbf{C}(e^{j\omega})$. The agreement between these two sets of responses is generally good below 6 kHz except for the back loudspeaker. This is because the inverse filters are gain-limited in the frequencies at which the plants have significant roll-off.

Next, the scenario of two passengers sitting in the FL and BR seats is examined. The preceding design procedure of inverse filers is employed in the HIF2 method. These plots are arranged in matrix form, where the ijth ($i = 1 \sim 4, j = 1, 2$) entry represents the respective inverse filter in (11). Similar to the result for a single passenger, the frequency response of inverse filters exhibit high gain in high frequencies. Figures 10(a) and 10(b) compare the plant-filter product and the matching model for the frontal and the back virtual images, respectively. Both the ipsilateral and contralateral responses of the plant-filter product did not fit the matching model responses very well. This is due to the fact that it is difficult to invert the nonsquare 4×2 acoustical plant matrix $\mathbf{H}$. A further comparison of the HIF2 and HIF2-S methods will be presented in the following subjective tests.

4.1.2. The Point-Receiver-Based Model. First, the scenario of a single passenger sitting in the FL seat is examined. Figure 11 shows the frequency responses between the four loudspeakers and the microphone placed at the center position of passenger's head (the control point). Figures 11(a) and 11(b) show the measured and the smoothed frequency responses of the acoustical plants when the FL and the FR loudspeakers are enabled. Figures 11(c) and 11(d) show the measured and the smoothed frequency responses of the acoustical plants when the BL and BR loudspeakers are enabled, respectively. Both the measured frequency responses were smoothed out by using the technique developed by Hatziantoniou and Mourjopoulos [23]. Similar to the results of the preceding HRTF-based approach, the frequency response of the filters

Table 2: The descriptions of four subjective listening experiments.

Experiment	I	II
Input content	5.1-channel	5.1-channel
No. passenger	1	2
Processing method	DWD	DWD
	HIF1	HIF2
	PIF1	HIF2-S
		PIF2-S
Reference	$FL_{\text{in}} + 0.7 \times C_{\text{in}} \rightarrow FL_{\text{out}}$	
	$FR_{\text{in}} + 0.7 \times C_{\text{in}} \rightarrow FR_{\text{out}}$	
	$BL_{\text{in}} \rightarrow BL_{\text{out}}$	
	$BR_{\text{in}} \rightarrow BR_{\text{out}}$	
Anchor	Summation of all lowpass filtered inputs → All outputs	

Table 3: The definitions of the subjective attributes.

Attribute	Description
Preference	Overall preference in considering timbral and spatial attributes
Fullness	Dominance of low-frequency sound
Brightness	Dominance of high-frequency sound
Artifacts	Any extraneous disturbances to the signal
Localization	Determination by a subject of the apparent source direction
Frontal	The clarity of the frontal image or the phantom center
Proximity	The sound is dominated by the loudspeaker closest to the subject
Envelopment	Perceived quality of listening within a reverberant environment

Table 4: The summary of the rendering strategies recommended for various listening scenarios.

Passenger		Number input channel	Strategy
1	FL	4	HIF1
1	BR	4	PIF1
2		4	DWD

shows high gain above 10 kHz due to the high-frequency roll-off of the back loudspeakers. Figure 12 shows the inverse plant-filter product, $H(e^{j\omega})C(e^{j\omega})$. The responses are generally in good agreement below 10 kHz except for the back loudspeakers.

4.2. Subjective Experiments. Subjective listening experiments were conducted to investigate the six audio rendering methods presented in Sections 2 and 3, according to a modified double-blind Multi-Stimulus test with Hidden Reference and a hidden Anchor (MUSHRA) [24]. The case designs of experiments are described in Table 2. In these experiments, four 5.1-channel music videos and a movie in Dolby Digital format were used. In the ("Dragon heart") movie, a scene with the dragon flying in a circle as a moving sound source is selected to be the stimulus for evaluating the attribute *localization*.

Eight subjective attributes employed in the tests, including *preference*, the timbral attributes (*fullness*, *brightness*, *artifact*) and the spatial attributes (*localization*, *frontal image*, *proximity*, *envelopment*) are summarized in Table 3. Forty subjects participating in the listening tests were instructed with definitions of the subjective attributes and the procedures before the tests. The subjects were asked to respond in a questionnaire after listening, with the aid of a set of subjective attributes measured on an integer scale from −3 to 3. Positive, zero, and negative scores indicate perceptually improvement, no difference, and degradation, respectively, of the signals processed by the rendering algorithm under test. The order to grade the attributes is randomized except that the attribute *preference* is always graded last. In order to access statistical significance of the test results, the scores were further processed by using the MANOVA. If the significance level is below 0.05, the difference among all methods is considered statistically significant and will be processed further by the Fisher's LSD *post hoc* test to perform multiple paired comparisons.

4.2.1. Experiment I

Methods. Experiment I is intended for evaluating the rendering algorithms designed for one passenger in the FL seat or BR seat. The DWD, HIF1, and PIF1 methods are compared in this experiment. Because only four loudspeakers are available in this car, the center channel of the 5.1-channel input is attenuated by −3 dB and mixed into the frontal channels to serve as the hidden reference. In addition, the four channels of input signals are summed and lowpass filtered (with 4 kHz cutoff frequency) to serve as the anchor.

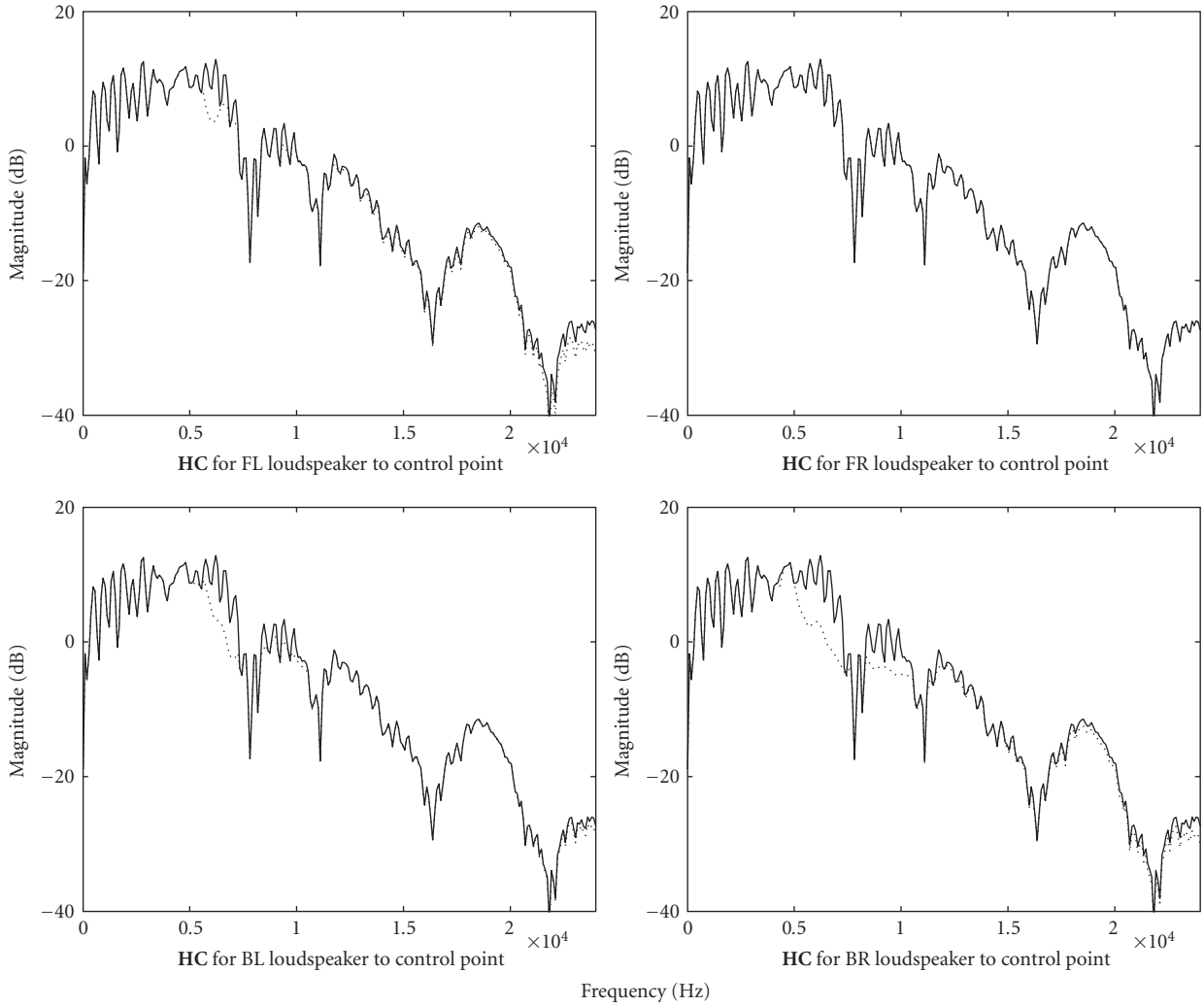

Figure 12: The comparison of frequency response magnitudes of the point-receiver-based plant-filter product and the matching model for single passenger sitting in the FL seat. The solid lines and the dotted lines represent the matching model responses **M** and the plant-filter product **HC**, respectively.

Results. Figures 13(a) and 13(b) show the means and spreads of the grades on the subjective attributes for the FL position, while Figures 13(c) and 13(d) show the results for the BR position. For the FL position, the results of the *post hoc* test indicate that the grades of the HIF1 method in *preference* and *fullness* are significantly higher than those of the DWD and the PIF1 methods. In *brightness*, only the grade of PIF1 methods is significantly higher than the hidden reference, while no significant difference between the DWD method and the HIF1 method is found. In addition, there is no significant difference among methods in the attributes *artifact*, *localization*, *proximity* and *envelopment*. In the attribute *frontal*, however, the inverse filter-based methods received significantly higher grades than the hidden reference and the DWD method.

In the BR position, there is no significant difference among all the methods in *fullness*, *artifact,* and *localization*. However, the grades received in *preference* and *brightness* using the inverse filtering-based method is significantly higher than the grades obtained using the other methods. In addition, all rendering methods received significantly higher grades in *proximity* than the hidden reference. Finally, only the HIF1 method significantly outperformed the hidden reference in *envelopment*. In general, all grades received are higher for the back seat than for the front seat. The HIF1 method received the highest grades in most attributes, especially in the spatial attributes. Considering the computation complexity, the PIF1 method is also a viable approach second to the HIF1 method because it received high grades in many attributes as well.

4.2.2. Experiment II

Methods. Experiment II is intended for evaluating the rendering algorithms designed for two passengers in the FL seat and BR seat and the 5.1-channel input. Four methods including the DWD method, the HIF2 method, the HIF2-S method, and the PIF2-S method are compared in

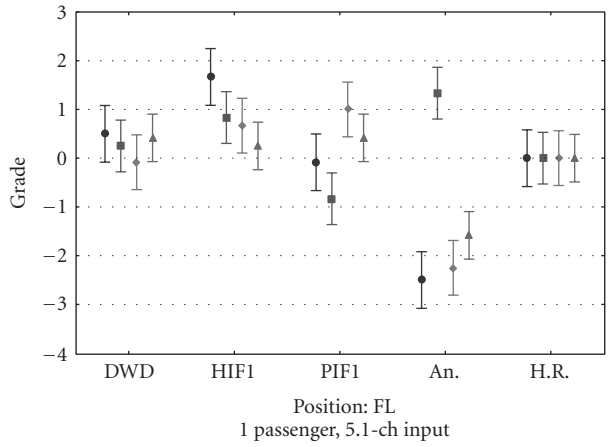

(a))The first four attributes for the FL seat.

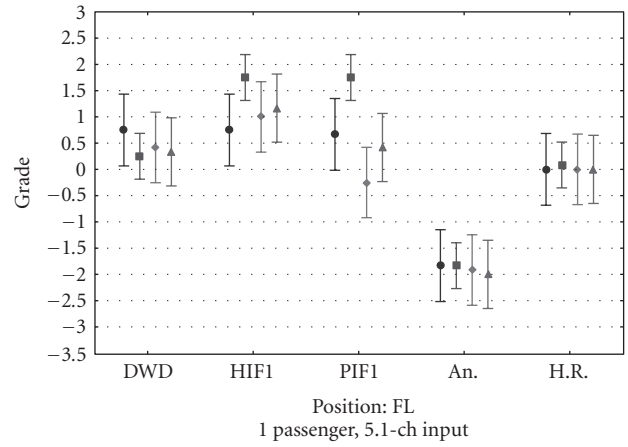

(b) The last four attributes for the FL seat.

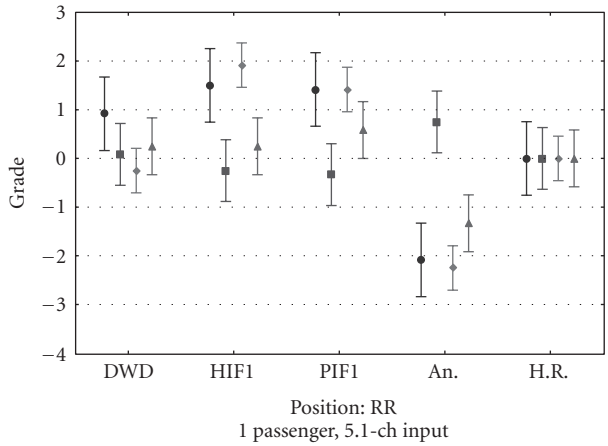

(c) The first four attributes for the RR seat.

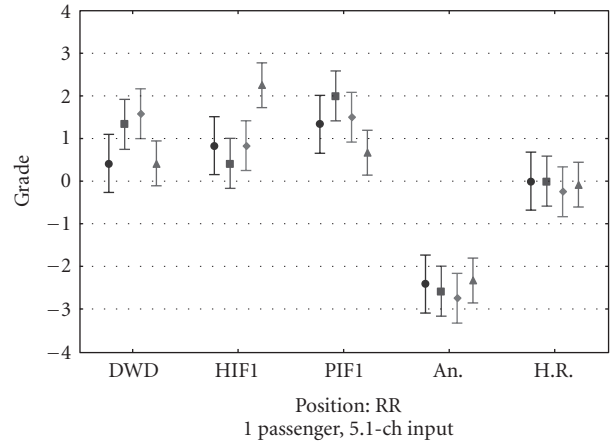

(d) The last four attributes for the RR seat.

Figure 13: The means and spreads (with 95% confidence intervals) of the grades on the subjective attributes for Experiment I.

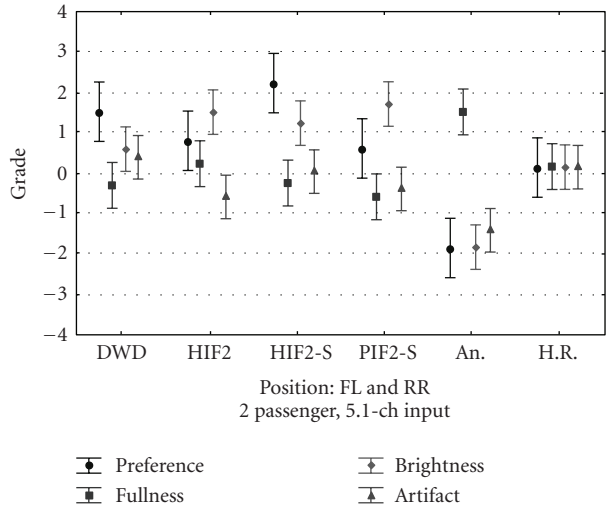

(a) The first four attributes.

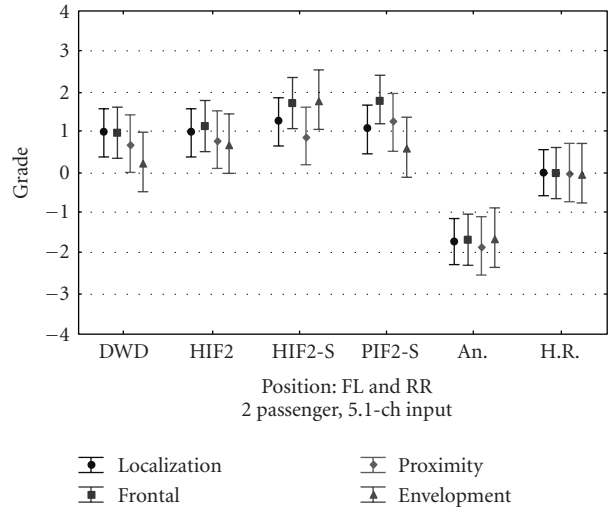

(b) The last four attributes.

Figure 14: The means and spreads (with 95% confidence intervals) of the grades on the subjective attributes for Experiment II.

this experiment. The hidden reference and the anchor are identical to those defined in Experiment I.

Results. Figure 14 shows the means and spreads of the grades of all subjective attributes. The results of the *post hoc* test reveals that there is no significant difference between the DWD method and HIF2-S method, while both grades in *preference* are significantly higher than the hidden reference. In *fullness* and *proximity*, no significant difference was found among all proposed methods. In *brightness*, results similar to Experiment I are obtained. The inverse filtering-based methods received significant higher grades than the hidden reference, albeit there is no significant difference among the inverse filtering-based methods methods. The HIF2 method received very low grade in *artifact*, implying that artifacts are audible. This could be due to the problem of inverse filter design for the nonsquare acoustical system. In *frontal* and *localization*, all methods received significantly higher grades than the hidden reference. Finally, the HIF2-S method has attained the best performance in *envelopment* among all methods. Overall, the HIF2-S method is the preferred choice for spatial quality, which is contrary to our expectation that more inverse filters (HIF2) should yield better performance. On the other hand, in terms of computation complexity and rendering performance, the DWD method is an adequate choice for the two-passenger scenario.

5. Conclusions

A comprehensive study has been conducted to explore various automotive audio processing approaches. Table 4 summarizes the conclusions on rendering strategies which can be drawn from the performed listening tests according to the number of passengers.

First, for the rendering scenario with a single passenger and the 5.1-channel inputs, the HIF1 method is suggested for the passenger sitting in the FL seat, whereas the PIF1 method would be the preferred choice for the passenger sitting in the BR seat. Second, for the two-passenger scenario, the HIF2-S method received high grade in most subjective attributes. However, no significant difference in the attributes *preference, brightness, artifact, localization* and *frontal* was found between the DWD method and the HIF2-S method. Considering the computational complexity, the DWD method should be the most preferred choice for the two-passenger scenario. Overall, the inverse filtering approaches did not perform as well for the multipassenger scenario as it did for the single passenger scenario. The number of inverse filters increases drastically with number of passengers, rendering approaches of this kind impractical in automotive applications.

Acknowledgments

The work was supported by the National Science Council in Taiwan, China, under the project no. NSC91-2212-E009-032.

References

[1] Y. Kahana, P. A. Nelson, and S. Yoon, "Experiments on the synthesis of virtual acoustic sources in automotive interiors," in *Proceedings of the 16th International Conference on Spatial Sound Reproduction and Applications of the Audio Engineering Society*, Paris, France, March 1999.

[2] B. Crockett, M. Smithers, and E. Benjamin, "Next generation automotive sound research and technologies," in *Proceedings of the 120th Convention of Audio Engineering Society*, Paris, France, 2006, paper no. 6649.

[3] M. R. Bai and C. C. Lee, "Comparative study of design and implementation strategies of automotive virtual surround audio systems," to appear in *Journal of the Audio Engineering Society*.

[4] P. Damaske and V. Mellert, "A procedure for generating directionally accurate sound images in the upper-half space using two loudspeakers," *Acoustica*, vol. 22, pp. 154–162, 1969.

[5] D. R. Begault, *3-D Sound for Virtual Reality and Multimedia*, AP Professional, Cambridge, Mass, USA, 1994.

[6] W. G. Gardner, "Transaural 3D audio," Tech. Rep. 342, MIT Media Laboratory, 1995.

[7] M. R. Bai and C.-C. Lee, "Development and implementation of cross-talk cancellation system in spatial audio reproduction based on subband filtering," *Journal of Sound and Vibration*, vol. 290, no. 3-5, pp. 1269–1289, 2006.

[8] M. R. Bai and C.-C. Lee, "Objective and subjective analysis of effects of listening angle on crosstalk cancellation in spatial sound reproduction," *The Journal of the Acoustical Society of America*, vol. 120, no. 4, pp. 1976–1989, 2006.

[9] M. R. Bai, G.-Y. Shih, and C.-C. Lee, "Comparative study of audio spatializers for dual-loudspeaker mobile phones," *The Journal of the Acoustical Society of America*, vol. 121, no. 1, pp. 298–309, 2007.

[10] T. Takeuchi and P. A. Nelson, "Optimal source distribution for binaural synthesis over loudspeakers," *The Journal of the Acoustical Society of America*, vol. 112, no. 6, pp. 2786–2797, 2002.

[11] D. Menzies and M. Al-Akaidi, "Nearfield binaural synthesis and ambisonics," *The Journal of the Acoustical Society of America*, vol. 121, no. 3, pp. 1559–1563, 2007.

[12] P.-A. Gauthier, A. Berry, and W. Woszczyk, "Sound-field reproduction in-room using optimal control techniques: simulations in the frequency domain," *The Journal of the Acoustical Society of America*, vol. 117, no. 2, pp. 662–678, 2005.

[13] T. Betlehem and T. D. Abhayapala, "Theory and design of sound field reproduction in reverberant rooms," *The Journal of the Acoustical Society of America*, vol. 117, no. 4, pp. 2100–2111, 2005.

[14] G. Theile and H. Wittek, "Wave field synthesis: a promising spatial audio rendering concept," *Acoustical Science and Technology*, vol. 25, no. 6, pp. 393–399, 2004.

[15] Pioneer, "MCACC Multi-Channel Acoustic Calibration," August 2008, http://www.pioneerelectronics.com/PUSA/PressRoom/Press+Releases/Car+Audio+Video/Computer+Technology+and+Car+Audio+Converge+in+Pioneer+Single+with+Hard+Disk+Drive%2C+Memory+Stick%2C+MP3+Playback.

[16] M. R. Bai and G.-Y. Shih, "Upmixing and downmixing two-channel stereo audio for consumer electronics," *IEEE Transactions on Consumer Electronics*, vol. 53, no. 3, pp. 1011–1019, 2007.

[17] S. Sharma, *Applied Multivariate Techniques*, John Wiley & Sons, New York, NY, USA, 1996.

[18] ITU-R Rec. BS.775-1, "Multi-channel stereophonic sound system with or without accompanying picture," International Telecommunications Union, Geneva, Switzerland, 1994.

[19] W. G. Gardner and K. D. Martin, "KEMAR HRTF measurements," MIT's Media Lab, August 2008, http://sound.media.mit.edu/resources/KEMAR.html.

[20] W. G. Gardner and K. D. Martin, "HRTF measurements of a KEMAR," *The Journal of the Acoustical Society of America*, vol. 97, no. 6, pp. 3907–3908, 1995.

[21] B. Noble, *Applied Linear Algebra*, Prentice-Hall, Englewood Cliffs, NJ, USA, 1988.

[22] P. D. Hatziantoniou and J. N. Mourjopoulos, "Errors in real-time room acoustics dereverberation," *Journal of the Audio Engineering Society*, vol. 52, no. 9, pp. 883–899, 2004.

[23] P. D. Hatziantoniou and J. N. Mourjopoulos, "Generalized fractional-octave smoothing of audio and acoustic responses," *Journal of the Audio Engineering Society*, vol. 48, no. 4, pp. 259–280, 2000.

[24] ITU-R BS.1534-1, "Method for the subjective assessment of intermediate sound quality (MUSHRA)," International Telecommunications Union, Geneva, Switzerland, 2001.